Silica Subsurface Amine Effect on the Chemical Stability and Chromatographic Properties of End-Capped Immobilized Artificial Membrane Surfaces

Robert J. Markovich, Xiaoxing Qiu, David E. Nichols, and Charles Pidgeon*

Department of Medicinal Chemistry, Purdue University, West Lafayette, Indiana 47907

Ben Invergo[1]

Regis Chemical Company, 8210 Austin Avenue, Morton Grove, Illinois 60053

Francisco M. Alvarez

Schering Plough Research, 2000 Galloping Hill Road, Kenilworth, New Jersey 07033

The silica surface of immobilized artificial membranes containing phosphatidylcholine (IAM.PC) has approximately two aminopropyl groups per immobilized phosphatidylcholine molecule. Primary amines near the silica subsurface adsorb biomolecules and also decrease the chemical stability of IAM.PC surfaces. Consequently, subsurface amines were end-capped by several methods including silylating reagents, acetyl analogues, glycidol, methyl glycolate, short-chain anhydrides (3-6 carbons/anhydride chain), and long-chain anhydrides (10-12 carbons/anhydride chain). All end-capping reactions resulted in loss of the initially immobilized phosphatidylcholine molecule. However, the amount of PC loss during end capping was very low (for alkyl anhydride end-capping reactions) to very high (for silylation end-capping reactions). After end capping, IAM.PC showed increased chemical stability compared to non end-capped IAM.PC surfaces. The chemical stability of IAM packing material was monitored by phospholipid leaching from IAM surfaces exposed to organic and aqueous solvents using thin-layer chromatography, ^{1}H NMR spectroscopy, infrared spectroscopy, and mass spectrometry. IAM.PC packing material end capped with long-chain anhydrides exhibited the greatest chemical stability, i.e., little or no detectable phospholipid leaching when challenged with aqueous and/or organic solvents. The chromatography of acidic and basic compounds on end-capped and non-end-capped IAM.PC surfaces was studied. Compared to non-end-capped IAM.PC HPLC columns, the chromatographic retention times of acidic compounds (deoxynucleotides) decreased after end capping. In contrast, the retention times of basic compounds (amphetamine analogues) increased on end-capped IAM.PC HPLC columns relative to non-end-capped IAM.PC HPLC columns. This indicates that these solutes have access to the silica subsurface amines during chromatography.

INTRODUCTION

Solid surfaces denoted as immobilized artificial membranes (IAMs) are rapidly evolving as a useful method to purify biomolecules, particularly membrane proteins (*1*, *2*). IAM surfaces have been used to purify (i) a cholesterol binding protein found in rat intestinal cells (*3*), (ii) the red blood cell glucose transporter (*4*), (iii) adrenal cytochrome P450 (*5*), and (iv) several cytochrome P450 isozymes from kidney, liver, insects, and cancer cells (*6*). IAM surfaces are also denoted as a solid-phase membrane mimetic because IAM surfaces are intended to emulate the lipid environment of cell membranes (*7-10*).

Scheme I. General Structure and Potential Chemical Degradation Sites of IAM Surfaces[a]

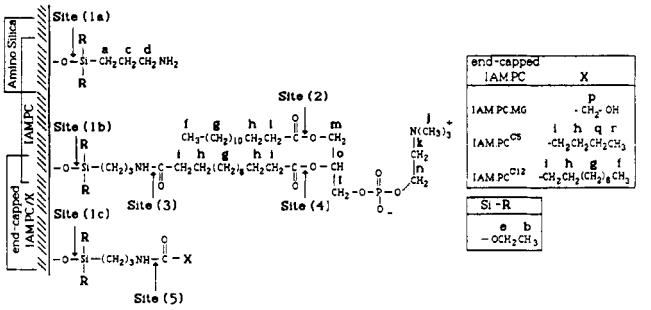

[a] ^{1}H NMR peak assignments are shown in Figure 6.

To date, all IAM surfaces utilize silica propylamine as the mechanically stable rigid surface for immobilizing membrane lipids (*7-9*). The molecular area of membrane lipids, e.g., diacylphosphatidylcholine (PC), is greater than the molecular area of propylamine tethered to the silica surface (*7*). Consequently, after coupling large-size PC molecules to silica propylamine, residual propylamine groups exist (Scheme I). Immobilized diacylated phospholipids with 14 carbons/alkyl chain project approximately 15 Å from the silica surface; thus, residual propylamine groups reside 15 Å below the immobilized phospholipid headgroups (*8*). Double-coupling PC to the silica propylamine surface increases the surface coverage of PC and decreases the number of residual amines; however, residual propylamine groups remain near the silica subsurface (*7*). Infrared (IR) analysis of IAM.PC surfaces perfused with citric acid buffered mobile phase indicated that citric acid is irreversibly bound to the propylamines (*9*). More recently, we found that residual surface amines are the primary cause of the chemical instability of IAM surfaces. Eliminating residual surface amines is thus necessary to improve the chemical stability of IAM chromatographic surfaces. In this report, we describe useful chemistry for end capping residual surface amines on IAM.PC bonded phases. In addition, the chromatography of acidic and basic compounds on end-capped and non-end-capped IAM.PC HPLC columns is described.

Abbreviations. The following abbreviations are used throughout this paper: BROSC, 3,5-dimethoxy-4-bromo-

* Author to whom correspondence should be addressed.
[1] Current address: Rhone-Poulenc, 9800 Blue Grass Parkway, Jeffersontown, KY 40299.

0003-2700/91/0363-1851$02.50/0

phenethylamine; 4-Br-TMA, 3,5-dimethoxy-4-bromophenylisopropylamine; BSTFA, bis(trimethylsilyl)trifluoroacetamide; BUSC, 3,5-dimethoxy-4-(*n*-butoxy)phenethylamine; C2 anhydride, acetic anhydride; C3 anhydride, propionic anhydride; C4 anhydride, butyric anhydride; C5 anhydride, valeric anhydride; isoC4 anhydride, isobutyric anhydride; C6 anhydride, hexanoic anhydride; C10 anhydride, decanoic anhydride; C12 anhydride, dodecanoic anhydride; CDI, carbonyldiimidazole; 2C-T, 2,5-dimethoxy-4-(methylthio)phenethylamine; d-ATP, deoxyadenosine triphosphate; d-CTP, deoxycytidine triphosphate; d-GTP, deoxyguanosine triphosphate; d-TTP, deoxythymidine triphosphate; 3,4-DMA, 3,4-dimethoxyphenylisopropylamine; 2,5-DMA, 2,5-dimethoxyphenylisopropylamine; DMAP, (dimethylamino)pyridine; DOB, 2,5-dimethoxy-4-bromophenylisopropylamine; DOET, 2,5-dimethoxy-4-ethylphenylisopropylamine; DOM, 2,5-dimethoxy-4-methylphenylisopropylamine; DON, 2,5-dimethoxy-4-nitrophenylisopropylamine; DOT, 2,5-dimethoxy-4-(methylthio)phenylisopropylamine; DSS, sodium 2,2-dimethyl-2-silapentane-5-sulfonate; DTE, dithioerythritol; DTT, dithiothreitol; ESC, 3,5-dimethoxy-4-ethoxyphenylethylamine; GPC, L-(α-glyceryl)phosphocholine; HMDS, hexamethyldisilazane; Hydrox-sil, hexamethyldisilazane–trimethylchlorosilane–pyridine (1:1:1); IAM, immobilized artificial membrane; IAM.FA, IAM surface containing a long-alkyl-chain fatty acid covalently linked to silica such that the carboxyl group is exposed to the mobile phase; IAM.PC, IAM surface containing a dimyristoylphosphatidylcholine analogue covalently linked to silica through an amide link; IAM.PC^{C2}, IAM.PC surface end capped with acetic anhydride; IAM.PC^{C3}, IAM.PC surface end capped with propionic anhydride; IAM.PC^{ISOC4}, IAM.PC surface end capped with isobutyric anhydride; IAM.PC^{C4}, IAM.PC surface end capped with butyric anhydride; IAM.PC^{C5}, IAM.PC surface end capped with valeric anhydride; IAM.PC^{C6}, IAM.PC surface end capped with hexanoic anhydride; IAM.PC^{C10}, IAM.PC surface end capped with decanoic anhydride; IAM.PC^{C12}, IAM.PC surface end capped with dodecanoic anhydride; IAM.PC.MG, IAM.PC surface end capped with methyl glycolate; ISOPROSC, 3,5-dimethoxy-4-(isopropyloxy)phenethylamine; lecithinCOOCH$_3$, 1-myristoyl-2-[(13-carboxymethyl)tridecanoyl]-*sn*-3-glycerophosphocholine; lecithinCOOH, 1-myristoyl-2-(13-carboxyltridecanoyl)-*sn*-3-glycerophosphocholine; MESC, mescaline; MG, methyl glycolate; MMPC, 1-myristoyl-*sn*-glycerophosphocholine (lysolecithin); PC, phosphatidylcholine; PMA, *p*-methoxyphenylisopropylamine; PROSC, 3,5-dimethoxy-4-(*n*-propoxy)phenethylamine; TFA, trifluoroacetic acid; TMA-2, 2,4,5-trimethoxyphenylisopropylamine; TMCS, trimethylchlorosilane; TMS, tetramethylsilane.

EXPERIMENTAL SECTION

Materials. LecithinCOOH was synthesized in our lab (*7*). IAM.PC and IAM.PC.MG were obtained from Regis Chemical Company (Morton Grove, IL). All IAM high-performance liquid chromatography (HPLC) columns were packed in acetone at Regis. DMAP, CDI, acetic anhydride, and glycidol were purchased from Sigma Chemical Company (St. Louis, MO). Prior to use, DMAP was recrystallized from ethyl acetate and ethyl ether as described (*5*). Three silylating reagents were used: HYDROX-SIL, BSTFA (Regisil-RC-1), and BSTFA/10% TMCS (Regisil-RC-3). All silylating reagents were purchased from Regis. For these silylating reactions, TMCS is the catalyst. All anhydrides were purchased from Aldrich Chemical Co. (Milwaukee, WI). HPLC-grade heptane, acetyl chloride, $CDCl_3$, D_2O, DSS, MG, benzoic acid, and sodium benzoate were purchased from Aldrich. MeOH, THF, toluene, and NH_4OH were purchased from J.T. Baker (Phillipsburg, NJ). $CHCl_3$, concentrated acetic acid, $NH_4H_2PO_4$, and acetone were purchased from Mallinckrodt (Paris, KY). TFA was purchased from Pierce Chemical Co. (Rockford, IL). HPLC-grade hexane and acetonitrile were purchased from EM Science (Gibbstown, NJ). $CHCl_3$ and THF were dried as described earlier (*5*), whereas all other solvents were used as received. Citric acid, NH_4Cl, and phosphorus pentoxide were purchased from Fisher Scientific (Fair Lawn, NJ). Ninhydrin and Phospray were purchased from Supelco, Inc. (Bellefonte, PA). Kieselgel thin-layer chromatography (TLC) plates, (5 × 20 cm) precoated with silica gel 60 F_{254} of 0.25 mm thickness, were purchased from E. Merck (Darmstadt, FRG). Whatman TLC plates (20 cm × 20 cm, 0.125 mm thick) were obtained from Whatman LabSales (Hillsboro, OR). 1,12-Dodecandicarboxylic acid anhydride and IAM.FA were synthesized as described (*8*). Analogues of amphetamine include MESC, DON, 3,4-DMA, PMA, ESC, TMA-2, 2,5-DMA, ISOPROSC, PROSC, DOM, 2C-T, BROSC, DOT, BUSC, DOB, 4-Br-TMA, and DOET; these basic compounds were either obtained from the National Institute of Drug Abuse or synthesized in our lab by known methods. Silica propylamine, 5, 7, and 12 μm size, with 300-Å pores, was obtained from Regis or Macherey-Nagel (Duren, Germany). Silica propylamine purchased from Macherey-Nagel bears the trade name of Nucleosil.

Ninhydrin Analysis of IAM Powder. Ninhydrin was used to qualitatively determine when end-capping reactions were complete. IAM packing material (~1–2 mg) was placed in a test tube (13 × 100 mm), and 2–3 drops of Ninhydrin was added. The powder was allowed to air dry at room temperature (~2 h or overnight). Non-end-capped IAM.PC powder turns dark purple immediately, whereas end-capped IAM.PC powder remains white or turns a light pink depending on the extent of end capping.

Silylating End-Capping Reactions. IAM.PC was dried 24 h in a vacuum desiccator at room temperature over phosphorus pentoxide. Approximately 50 mg of packing material was suspended in 1 mL of distilled THF in a 3-mL-capacity microflex vial. Silylation reagents were chilled in a dry ice acetone bath and then added to the IAM suspension by using a syringe; the volumes were either 100 μL of BSTFA, 200 μL of HMDS–TMCS–pyridine, or 200 μL of BSTFA/10% TMCS. After 9 h, the reaction mixture was filtered (scintered glass M) and the IAM.PC powder was sequentially washed (25 mL/wash) with dry THF, acetonitrile, and acetone.

***N*-Acetyl End-Capping Reactions.** IAM.PC was end-capped by using either acetylimidazolide, acetic anhydride, or acetyl chloride. All reactions were protected from light and purged with nitrogen. Acetylimidazolide was synthesized by stirring acetic acid (30 mg, 0.49 mmol) and CDI (79.38 mg, 0.49 mmol) in dry $CHCl_3$ (7 mL) at room temperature for 2 h. IAM.PC (50 mg) was then added, and the suspension was stirred at room temperature for 18 h. Acetic anhydride (30 mg, 0.49 mmol) was stirred at room temperature with IAM.PC (50 mg) in dry $CHCl_3$ (10 mL) for 18 h. Similarly, acetyl chloride (30 mg, 0.38 mmol) was stirred at room temperature with IAM.PC (50 mg) in dry $CHCl_3$ (10 mL) for 18 h. Acetyl end-capping reactions were sequentially washed with 40 mL each of distilled $CHCl_3$ and THF.

MG and Glycidol End-Capping Reactions. MG (5 mL, 64.8 mmol) was refluxed (~100 °C) with IAM.PC (5 g) in toluene–heptane (150 mL–50 mL) for 48 h. MG and heptane are not miscible. Glycidol (15 mL, 226.2 mmol) was stirred with IAM.PC (5 g) at room temperature for 27 h. IAM.PC was washed 2 times with 100 mL of H_2O followed by washing with HPLC-grade MeOH. After end capping, the IAM packing material was washed with 150 mL of toluene and then 150 mL of hexane.

Anhydride End-Capping Reactions. IAM.PC (200–500 mg) was suspended in dry $CHCl_3$ (4–6 mL), and anhydrides were added to a final ratio of 0.09–0.12 mg of anhydride/mg of IAM.PC; there is ≥10-fold excess of anhydride. Reactions were purged with nitrogen, then sealed with a rubber septum, and gently stirred at room temperature for 18–24 h. At this time, the reaction mixture was centrifuged at ~1500 rpm and the $CHCl_3$ supernatant was removed but not discarded. The IAM.PC packing material was washed 3 times with ~7 mL each of $CHCl_3$, THF, and acetone. The THF wash was necessary to remove all adsorbed fatty acid and unreacted anhydride.

Thin-Layer Chromatography. Lipids that leach from the IAM surface were identified by both TLC and mass spectrometry (MS). IAM.PC (1 g) and IAM.PC.MG (0.9 g) were extracted in separate test tubes to obtain enough lipid for TLC and MS analysis as follows. IAM packing material was suspended in 6 mL of $CHCl_3$/MeOH (2:1 v/v) and briefly vortexed (~15–30 s)

followed by centrifugation (~5 min, 1500 rpm). IAM.PC was suspended, vortexed, and pelleted 6 times by using this procedure, and the supernatants were pooled and rotoevaporated to dryness. The residue was suspended in $CHCl_3$, filtered, concentrated by a stream of nitrogen gas, and quantitatively applied to a 20-cm × 20-cm analytical TLC plate. After solvent development, a 2-cm column of the TLC plate was cut off with a glass cutter and sprayed with Phospray to identify the phosphate positive spots. The unsprayed TLC plate was then scrapped at retardation factor (R_f) values corresponding to each lipid. Lipids exibiting a high R_f value ($R_f > 0.15$) were extracted with $CHCl_3$/MeOH (2:1 v/v), whereas lipids with a low R_f value ($R_f < 0.15$) were extracted with MeOH. The extracted samples were evaporated to dryness and analyzed by MS. After MS, the samples werre subjected to TLC analysis to confirm purity. All phospholipids purified by TLC and analyzed by MS were a single spot when rechromatographed under the same TLC conditions used to purify the lipids. All TLC was performed with a 65:25:4 $CHCl_3$/MeOH/H_2O solvent system.

Elemental Analysis and Mass Spectrometry. Elemental analysis was performed on a Perkin-Elmer PE 240 and a Seargent manual apparatus at Purdue University's Chemistry Department in the Microanalysis Laboratory. Fast atom bombardment (FAB) using a 3:1 DTT/DTE matrix was performed on a Kratos MS50 mass spectrometer at Purdue University in the School of Pharmacy.

Infrared Spectroscopy. Complete details of the infrared equipment in our lab have been described (*7–12*). All infrared measurements of IAM silica were obtained by using an infrared microscope in the reflectance mode and a gold sample mirror. Infrared reflectance spectroscopy has been extensively used to study silica and modified silica surfaces (*7–9, 12–22*), and our infrared method to quantitate immobilized lipids has recently been described (*8, 9, 12*). The formation of IAM silica wafers was required for reproducible band intensities that are necessary for quantitative IR studies (*18–29*). Silica was compressed into wafers (~50 μm thick and 3 mm in diameter) prior to IR measurements. The IR spectra, converted to absorbance units, are double-diffuse transmission measurements (i.e., the incident light penetrates through the sample to the mirror surface and is reflected back through the sample) because the wafers were less than 100 μm thick (*24, 29, 30*). Infrared spectra were taken at 8-cm^{-1} resolution, and the spectra were not smoothed. Interferograms from 128 scans were coadded and apodized with a Happ-Genzel function before Fourier transformation. Useful spectral information of IAM surfaces can only be obtained in the IR region between 4000 and 1400 cm^{-1} because of intense silica oxide vibrations below 1400 cm^{-1} (*12, 13, 31–33*).

Several "lipid" IR band areas were integrated by using a computer program written by us for Nicolet SX software (*11, 12*). The limits for integration were as follows: hydrocarbon area $\bar{\nu}$ = 2995–2825 cm^{-1}; ester area $\bar{\nu}$ = 1775–1700 cm^{-1}; and amide I area $\bar{\nu}$ = 1690–1590 cm^{-1}. However, each of these lipid IR band areas were normalized by dividing by the area under the $\bar{\nu}_c$(SiO) band centered at 1870 cm^{-1} (*8, 9, 12, 18–22*). The area under the $\bar{\nu}_c$(SiO) band was integrated from $\bar{\nu}$ = 1945 to 1780 cm^{-1}. Normalizing each lipid band area to the $\bar{\nu}_c$(SiO) band in each spectra allowed direct comparison of all bonded phases (*8, 9, 12, 18–22*). The normalized hydrocarbon is directly proportional to the % C determined by elemental analysis (*8*). Consequently, we routinely calculate the hydrocarbon content (% HC) of IAM surfaces by using infrared analysis instead of elemental analysis. The % HC accuracy by infrared analysis is ±0.2% HC and % C accuracy by elemental analysis is ±0.2% C (*8*).

Three different silica propylamines, whereby the % C differed by a factor of 3, were exhaustively reacted with 1,12-dodecanedicarboxylic acid anhydride to synthesize IAM.FA. The normalized amide I area of the IAM.FA surface was directly proportional to the % C determined by elemental analysis (not shown). Thus, the amide I area can be used to quantitatively determine the amount of propylamines converted into amides by end capping with anhydrides.

As shown in Scheme I, cleavage site 2 causes the loss of only one immobilized ester without the concomitant loss of the immobilized PC headgroup. However, cleavage at sites 1b, 3, and 4 results in the loss of both the immobilized PC headgroup and the two immobilized PC ester groups. The ester area was thus used to estimate the amount of PC headgroups remaining on the IAM surface. For example, if 10% of the esters were lost during end capping with anhydrides, then ~10% of the initially immobilized PC headgroups were lost during end capping. Ester areas are sensitive to the physical state of the ester, and this is an approximation.

High-Performance Liquid Chromatography. HPLC equipment in our lab has been described in detail (*7–9, 12*). Analytical-size IAM.PC and IAM.PC.MG columns, 4.6 × 150 mm, were used for chromatographic studies of deoxynucleotides and amphetamine analogues. Chromatography of deoxynucleotides used a mobile phase containing 35 mM citric acid, 35 mM $NH_4H_2PO_4$, and 35 mM NH_4Cl, pH adjusted to pH 4.8 with concentrated NH_4OH. Individual deoxynucleotides were dissolved in the mobile phase at a final concentration of ~25 μg/mL. The deoxynucleotide solutions were injected (10–20 μL) every 200–500 mL during the continuous perfusion of 10000 mL of mobile phase. The column pressure increased (ca. 200–400 psi) during the perfusion of 10 L of mobile phase. Chromatography of amphetamine analogues used a mobile phase containing 0.1 M $NH_4H_2PO_4$ at pH 7.2. Stock solutions (1–2 mg/mL) of amphetamine analogues were prepared in this mobile phase and diluted with the same mobile phase to 0.01–0.1 μg/mL prior to injection (10–20 μL) at room temperature. The IAM column pressure varied between 900 and 1200 psi during the study.

^{1}H NMR Spectroscopy. ^{1}H NMR spectroscopy was used to evaluate lipids that leach from different IAM bonded phases exposed to both aqueous and organic solvents. IAM packing material (100 mg) and D_2O (700 μL) were briefly vortexed and then microfuged (10 min, 14000 rpm) in a 0.2-μm microfilterfuge tube. The D_2O aqueous filtrate (550 μL) was directly transferred to a 5-mm NMR tube; however, the IAM packing material was lyophilized and then extracted with 1 mL of $CHCl_3$/MeOH (2:1 v/v). The organic extract (800 μL) was evaporated to dryness and the residue dissolved in $CDCl_3$ (700 μL), and the ^{1}H NMR spectra were obtained in a 5-mm NMR tube.

All ^{1}H NMR spectra were obtained by accumulating 16 scans at 20 °C on a Varian VXR-500 spectrometer operating a proton frequencies of 500 MHz and a spectra width of 6000 Hz. Aqueous filtrate ^{1}H NMR spectra were referenced to the methyl protons at 0.00 ppm DSS. DSS was used as an external standard. The ^{1}H NMR spectra of the organic extracts were referenced to δ = 0.0 ppm using TMS as an internal standard. Chemical shift assignments were based on standard compounds (*34*). External standards were used to scale all of the ^{1}H NMR spectra: sodium benzoate (2.1 μmol/60 μL of D_2O) for the aqueous filtrate spectra, and benzoic acid (1.5 μmol/60 μL of $CDCl_3$) for the organic extract spectra. Water suppression, by presaturation of the HOD signal, was necessary for obtaining aqueous filtrate spectra.

RESULTS

IR spectra of IAM.PC end capped with three different silylation reagents demonstrated that the IAM surface was degraded during end capping. The hydrocarbon content decreased from 16.8% to 50% HC of the initial hydrocarbon loading (Table I). This hydrocarbon loss indicates that ~ 16.8–52% of the PC molecules leached during end capping.

In contrast to silylation reactions, infrared spectra demonstrated that end capping with either MG or glycidol does not destroy the IAM.PC surface. The symmetric and asymmetric CH stretch region ($\bar{\nu}$ = 2995–2825 cm^{-1}) increased in intensity (Figure 1), and the % C increased 39.3% and 27.1% for IAM.PC.MG and IAM.PC.glycidol surfaces, respectively (Table I). In addition, Figure 1 shows that a large increase in the intensity of the ester band occurred when the surfaces were end capped with MG. The increase in % HC on IAM.PC.MG was 158.6% HC. This exceeds the theoretical limit if only 1 mol of MG reacted with only 1 mol of residual amines. However, both elemental analysis (% C) and FTIR analysis (% HC) indicated that end capping exceeded 1 equiv. MS was necessary to determine the chemical reason for the consumption of more than 1 equiv of MG during end capping. IAM.PC.MG and IAM.PC.glycidol packing material were Ninhydrin negative or only very slightly Ninhydrin positive.

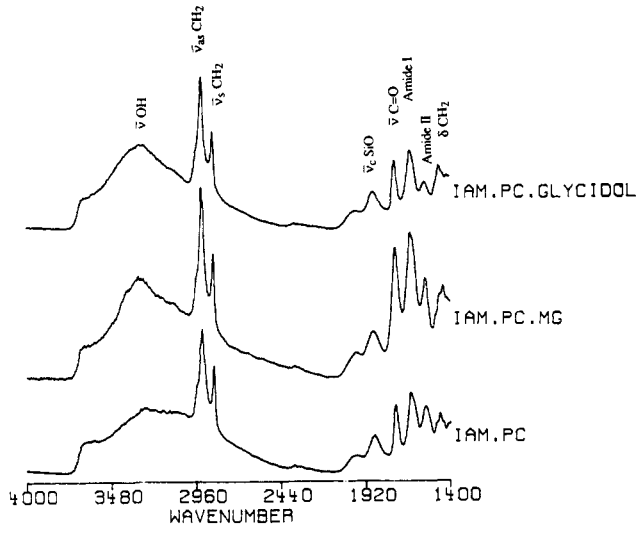

Figure 1. Infrared spectra of IAM.PC (12 μm) before and after end capping with MG and glycidol. Spectra are scaled to the $\bar{\nu}_c$(Si–O) band centered at 1870 cm^{-1}.

Both glycidol and MG were thus successful in end capping all of the residual surface amines on IAM.PC surfaces and therefore were packed into HPLC columns.

Figure 2 shows that the retention times of deoxynucleotides (acidic compounds) slowly decrease after repeated injections onto non-end-capped IAM.PC columns during the perfusion of 10 L of mobile phase. IAM.PC surfaces, perfused with citric acid mobile phases, slowly accumulate citric acid; this causes decreased retention of deoxynucleotides as the volume of mobile phase perfusing the column increases (*9*). The decreased retention times of deoxynucleotides on IAM.PC columns shown in Figure 2 are thus expected. However, the key concept in Figure 2 is that the retention times significantly decrease when the residual primary amines were reduced or eliminated by end capping. For example on new columns, the retention times of d-ATP are IAM.PC ~70 min, IAM.PC.glycidol ~35 min, and IAM.PC.MG ~2 min (see Figure 2A, first injection). Rank ordering the basicity of the silica surface gives

basic neutral

IAM.PC >>> IAM.PC.glycidol > IAM.PC.MG

and the elution of deoxynucleotides correlates with this basicity. In other words, all deoxynucleotides (i.e., acidic compounds) tested have the longest retention time on chemically basic IAM.PC columns and the shortest retention time on the chemically neutral IAM.PC.MG columns. Glycidol end capping reduces but does not eliminate the basicity of the silica subsurface, and consequently, the retention times of deoxynucleotides are reduced but not eliminated.

Figure 3 compares the retention times of 17 basic compounds on IAM.PC surfaces to the retention times on IAM.PC.MG. The silica propylamine starting material does not significantly influence the retention of basic compounds; IAM.PC/Nucleosil performs virtually identical with IAM.

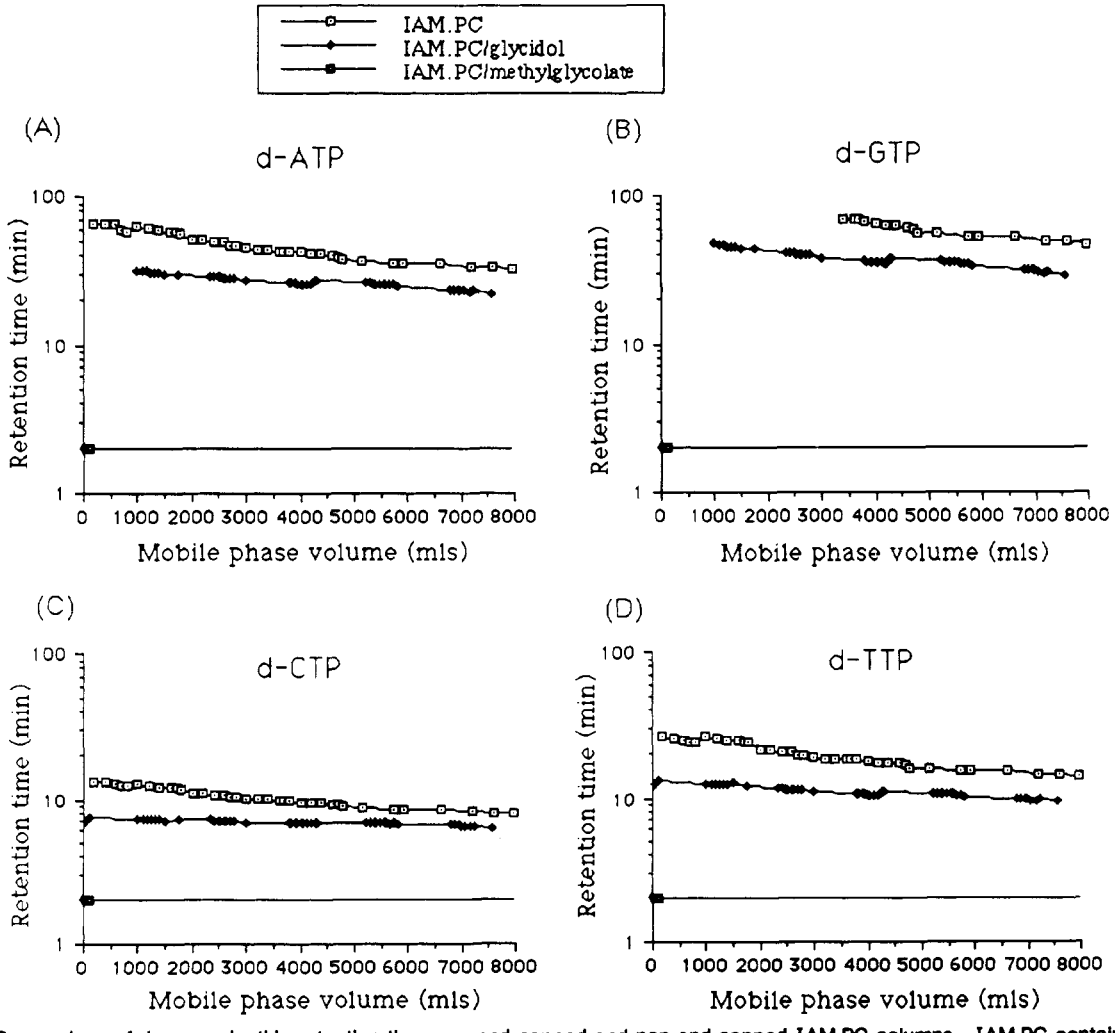

Figure 2. Comparison of deoxynucleotide retention times on end capped and non-end-capped IAM.PC columns. IAM.PC contains a primary amine near the silica subsurface. IAM.PC.glycidol contains secondary and tertiary amines near the silica subsurface. IAM.PC.MG is neutral.

Table I. % C or % HC Content of IAM.PC Packing Material before and after End Capping

IAM bonded phase	before end capping		after end capping		net diff[c]	
	% HC[a]	% C[b]	% HC[a]	% C[b]	% HC[a]	% C[b]
silylating reagents						
IAM.PC/BSTFA	5.18	N.D.	4.13	N.D.	-16.8	N.D.
IAM.PC/BSTFA-10% TMCS	5.18	N.D.	3.42	N.D.	-34.0	N.D.
IAM.PC/Hydrox-sil	5.18	N.D.	2.48	N.D.	-52.0	N.D.
non-silylating reagents						
IAM.PC.MG	N.D.	4.17	N.D.	5.81	N.D.	+39.3
IAM.PC.glycidol	N.D.	4.17	N.D.	5.30	N.D.	+27.1
IAM.PC/acetylimidazole	N.D.	4.95	N.D.	4.39	N.D.	-11.3
IAM.PC/acetic anhydride	N.D.	4.95	N.D.	4.53	N.D.	-7.9
IAM.PC/acetyl chloride	N.D.	4.95	N.D.	4.62	N.D.	-6.7

[a] Carbon content determined by infrared spectroscopy, i.e., % HC. [b] Carbon content determined by elemental analysis, i.e., % C. [c] Net difference = [% HC (or % C) after end capping - % HC (or % C) before end capping]/% HC (or % C) before end capping. Negative values indicate a net loss, while positive values indicate a net gain.

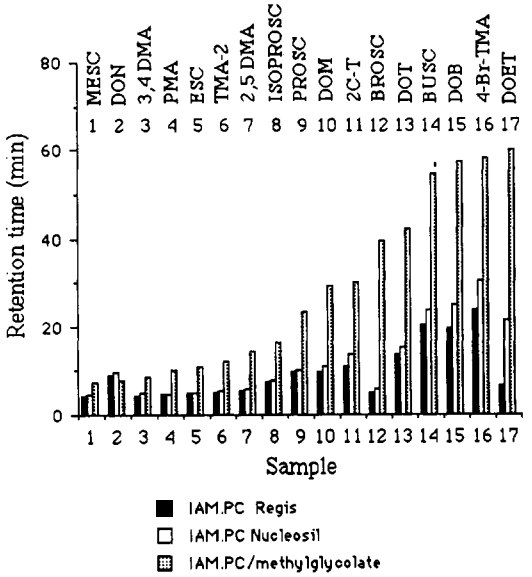

Figure 3. Increased retention of basic compounds on IAM.PC end capped with MG. All compounds were injected 2 or 3 times, and the average retention time is given. Compounds were rank ordered according to their retention on the IAM.PC.MG column. Two types of silica propylamine were used: Regis silica propylamine, which is 5 μm (i.e., IAM.PC/Regis), and Nucleosil, which is 7 μm (i.e., IAM.PC/Nucleosil). End capping IAM.PC/Regis with MG was used to obtain IAM.PC.MG.

Scheme II. IAM Surface Catalysis[a]

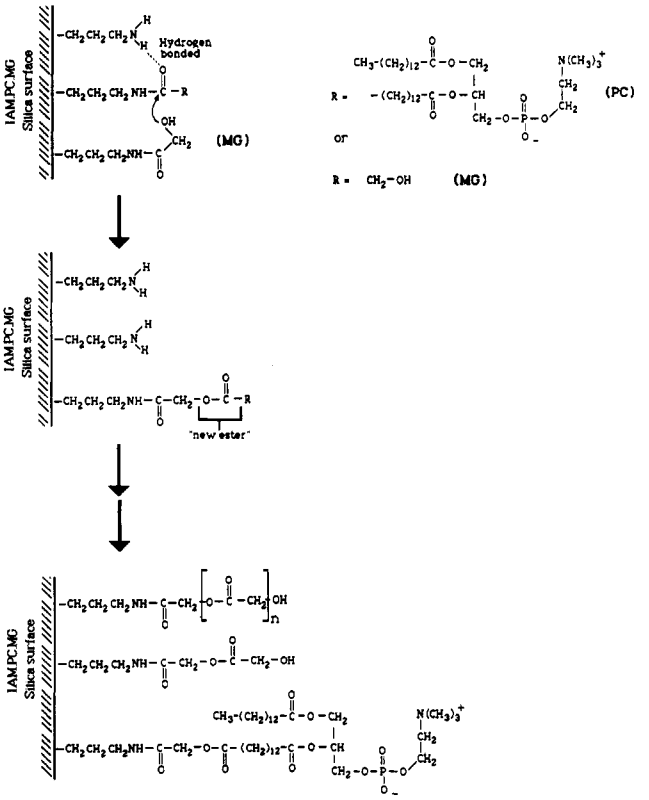

[a] Hydroxyl groups from immobilized MG attack neighboring amide bonds to transfer either MG or PC to the attacking MG hydroxyl group. This causes the formation of a new ester.

PC/Regis. However, both of these surfaces are chemically basic and the retention time of basic compounds is not expected to increase. In fact, these residual amines should actually decrease the binding of basic compounds. In other words, immobilized propylamine near the silica floor of IAM.PC decreases the retention time of basic solutes. As expected, the retention times of basic compounds increased when the silica propylamines were eliminated by end capping with MG (Figure 3).

MS was used to identify the lipids that leach from the two commercially available IAM surfaces: IAM.PC and IAM.PC.MG. In Figure 4, diacylated glycerophosphatidylcholine lipids include spots 5, 6, and 8 and the monoacylated glycerophosphatidylcholine lipids include spots 2–4. The phosphate positive spots 1 and 7 could not be identified. Spot 5 corresponds to lecithinCOOH initially tethered to the amino silica. The formation of lecithinCOOH is from the hydrolysis of the amide link (site 3 in Scheme I). Spot 6 corresponds to methanolysis of the amide link (site 3 in Scheme I). Spot 4 is the result of cleavage of site 4 (in Scheme I) and generates MMPC. The very weak phosphate positive spots (spots 2 and 3) are caused from cleavage of two bonds. Both spot 2 and spot 3 are derived from cleaving the *sn*-2 ester (site 2 in Scheme I), and the chemical difference between spot 2 and spot 3 resides in how the amide link was cleaved. Spot 3 was formed from "methanolysis" of the amide link, and spot 2 was generated from "hydrolysis" of the amide link. We note that spot 4 results from cleavage of the *sn*-2 ester (site 4, in Scheme I). It is thus not surprising that end capping with MG did not protect this site. On the basis of MS, cleavage of the amide link is responsible for 4 of the 6 lipids that leach from the IAM.PC surface (i.e., spots 2, 3, 5, and 6). End capping the IAM.PC surface with MG eliminated methanolysis of the amide link, i.e., both spot 3 and spot 6 are absent in the IAM.PC.MG TLC lane, but not hydrolysis because spots 2 and 5 are present in the IAM.PC.MG TLC lane (Figure 4).

The most interesting result from the analysis of leached lipids is the identification of spot 8, which leached from the IAM.PC.MG surface. MS demonstrated that this molecule

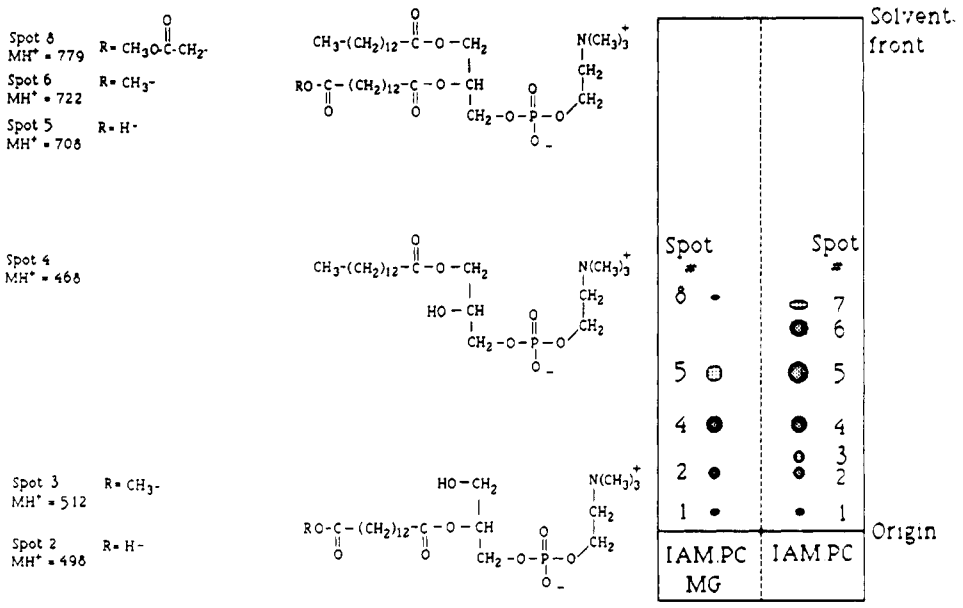

Figure 4. Mass spectrometric identification of lipids that leach from IAM.PC and IAM.PC.MG surfaces washed with $CHCl_3$/MeOH (2:1 (v/v)). Spot 1 and spot 7 could not be identified.

Table II. Infrared Characterization of IAM.PC Surfaces before and after End Capping

IAM packing material		% HC (% net HC)[a]	ester area (% PC)[b]	amide I area (% residual amines)[c]	Ninhydrin[d]
IAM.PC	reference	3.37	0.83	1.32 (+41.8)	purple
IAM.PC (stability test)	$CHCl_3$, 18 h[e]	3.19 (-5.3)	0.79 (-4.8)	1.41 (+38.0)	purple
IAM.PC^{C3}	1st end cap rxn	3.04 (-9.8)	0.64 (-22.9)	2.17 (+1.9)	light pink
IAM.PC^{C3}	2nd end cap rxn	3.15 (-6.5)	0.65 (-21.7)	2.27 (0.0)[f]	white[g]
IAM.PC^{C8}	1st end cap rxn	3.57 (+5.9)	0.62 (-25.3)	2.03 (+10.6)	light purple
IAM.PC^{C8}	2nd end cap rxn	3.56 (+5.9)	0.62 (-25.3)	2.06 (+9.25)	light pink/white
IAM.PC^{C12}	1st end cap rxn	3.78 (+12.1)	0.70 (-15.7)	1.85 (+22.7)	purple
IAM.PC^{C12}	2nd end cap rxn	3.88 (+15.13)	0.69 (-16.9)	1.93 (+15.0)	light pink
IAM.PC^{C12} (stability test)	$CHCl_3$, 18 h	3.85	0.68	1.95	light pink
IAM.PC[h]	reference	4.56	1.07	1.57	purple
IAM.PC glycidol[h]	1st end cap rxn	5.00 (+9.7)	1.06 (0.0)	1.75	white
IAM.PC.MG[h]	1st end cap rxn	11.79 (+158.6)	4.23 (+295.3)	6.01	white

[a] The % net HC was calculated from ([% HC(before end capping) - % HC(after end capping)]/% HC(before end capping))100. [b] The % PC remaining on the IAM surface after end capping or challenged with solvent was estimated from the following equation: ([ester area(before end capping) - ester area(after end capping)]/ester area(before end capping))100. [c] Double end capping with C3 anhydrides formed a Ninhydrin negative IAM surface, and therefore, the amide I area of IAM.PC^{C3} was used as the reference for calculating the % residual amines. The % residual amines was calculated as follows: ([amide I area(IAM.PC^{C3}) - amide I area(IAM surface)]/amide I area(IAM.PC^{C3}))100. [d] Ninhydrin was used to evaluate when end capping was complete, i.e., no residual amines existed on the IAM surface. [e] This stability test did not contain anhydride, and the $CHCl_3$ was distilled. [f] This Ninhydrin negative IAM surface has all residual amines converted into amides. The intensity of this amide I band was assumed to exhibit the maximum intensity, and therefore this amide I was used for calculating % residual amines for all anhydride end-capping reactions. [g] Double end-capping IAM.PC with all anhydrides rarely generates a packing material that remains bright white after 24 h in the Ninhydrin reagent. This sample remained bright white. The other end-capped packing material are very light pink after 24 h. [h] IAM.PC surfaces were obtained from the same synthetic batch followed by end capping with MG or glycidol. The IAM.PC used for these data was a different lot than the IAM.PC used for the anhydride reactions. Consequently, the % HC reference is different.

was formed from the reaction of the terminal carboxyl group on lecithinCOOH with the primary alcohol of MG. A possible mechanism for this reaction is shown in Scheme II. The primary alcohol from an immobilized MG attacks the neighboring amide bond that links PC to the silica surface. The reaction of the MG alcohol with the neighboring amide forms a "new ester" and a new primary amine on the silica surface. The amide bond link may or may not be hydrogen bonded to facilitate this reaction. The attack of the MG alcohol on the adjacent amide in principle can occur on any adjacent amide. Thus, the MG amide bond may also be cleaved by a neighboring MG alcohol. Scheme II shows that both MG and PC can be transferred to the adjacent amine with the formation of a new ester bond. This results in MG monomers, MG dimers, MG trimers, etc., during end capping with MG. This is consistent with the large increase in % C determined by elemental analysis (Table I) and in % HC determined by infrared analysis (Table II). This is also consistent with the large ester bands in the infrared spectra of IAM.PC.MG packing material shown in Figure 1; the IAM.PC.MG ester area $\bar{\nu}$(C=O) = 1741 cm^{-1}, is ~300 % greater than the ester area of IAM.PC packing material (Table II).

End capping with MG generates new hydroxyl groups near the silica surface. Biological and artificial membranes do not typically contain these functional groups in the hydrocarbon part of the bilayer. Consequently, we end capped the IAM.PC surface with anhydrides. Infrared spectra representative of end-capping IAM.PC with anhydrides are shown in Figure 5. Unlike the infrared spectra shown in Figure 1, the amide I band ($\bar{\nu}$ = 1650 cm^{-1}) is significantly larger than the lecithin ester band ($\bar{\nu}$(C=O) = 1742 cm^{-1}). Unexpectedly, the intensity and band shape of the amide I band ($\bar{\nu}$ = 1650 cm^{-1}), amide

	Amide A	Amide B	$\bar{\nu}_{as}$ CH_2	$\bar{\nu}_s$ CH_2	$\bar{\nu}_c$ Si(O	$\bar{\nu}$ C=O	Amide I	Amide II	δ CH_2
IAM.PC^{C12}	3286.2	3084.5	2927.6	2856.8	1873.6	1739.9	1643.3	1549.6	1465.4
IAM.PC^{C6}	3289.8	3084.9	2927.9	2857.7	1873.4	1740.3	1643.7	1549.7	1465.0
IAM.PC^{C3}	3300.1	3090.6	2928.0	2857.7	1872.6	1739.9	1643.6	1550.3	1464.9
IAM.PC	-	-	2927.5	2856.9	1871.6	1738.5	1643.1	1552.7	1467.7

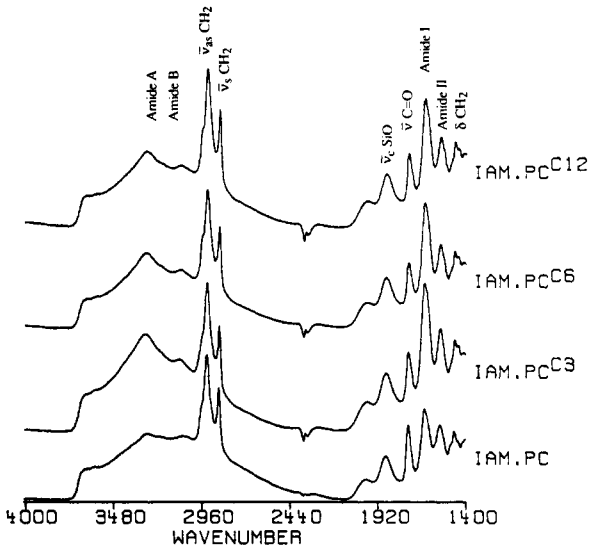

Figure 5. Infrared spectra of IAM.PC before and after end capping twice with anhydrides. Spectra are scaled to the $\bar{\nu}_c$(Si–O) band centered at 1870 cm^{-1}.

II band ($\bar{\nu}$ = 1550 cm^{-1}), and ester band ($\bar{\nu}$(C=O) = 1742 cm^{-1}) after deconvolution was independent of the anhydride used for end capping (not shown).

The % HC lost during stirring IAM.PC in $CHCl_3$ for 18 h (i.e., the stability test for IAM.PC, which mimics the end-capping reaction condition), was −5.3% HC (Table II). Consistent with this is the decreased ester area of −4.8% (Table II). Thus, without end capping the amount of lipid lost, measured by either the hydrocarbon area or the ester area, was virtually identical. During the first end-capping reaction with propionic anhydride, −9.8% HC was lost (Table II). After the first end-capping reaction with C6 and C12 anhydrides, a net gain of +5.9% and +12.1% HC respectively, was found on the IAM.PC surfaces. Thus, end capping IAM surfaces requires the alkyl chain length to be ≥ C6 anhydrides to have a net gain in % HC after end capping.

The extent of end capping, estimated by the amide I area, indicated that ~2%, 11%, and 22% of the propylamines existed after the first end-capping reaction with C3, C6, and C12 anhydrides, respectively (Table II, % residual amines). After the second end-capping reaction, the % residual amines was 0%, ~9%, and 15% for IAM.PC^{C3}, IAM.PC^{C6}, and IAM.PC^{C12}, respectively (Table II). Apparently end capping with C12 anhydrides cannot eliminate all residual amines, and this is most likely due to steric hindrance near the silica surface. However, end capping with C12 anhydrides followed by a second end-capping reaction with C3 anhydrides resulted in a Ninhydrin negative IAM.PC surface (not shown). Although double end capping with the C12 anhydride did not elicit a Ninhydrin negative IAM surface, the IR spectra of this surface showed no change after stirring in $CHCl_3$ for 18 h (stability test for IAM.PC^{C12}, Table II). In other words, the double-end-capped IAM.PC^{C12} surface is completely stable to the reaction conditions used to synthesize the surface. This is clearly evident by comparing the % HC, ester area, and amide I area of IAM.PC^{C12} to the other IAM surfaces listed in Table II. We note that all IAM.PC surfaces subjected to a second end-capping reaction using the same anhydride were significantly more stable during the second end-capping reaction; this is based on little or no phosphate positive spots appearing on TLC plates loaded with a large aliquot of the reaction/wash solvent.

Perfusing new IAM.PC.MG and IAM.PC guard columns with 100 mL of $CHCl_3$/MeOH (2:1 v/v) and subjecting the mobile-phase eluent to TLC analysis showed 4–5 phosphate positive spots in the thin-layer chromatogram. The entire 100-mL perfusate was evaporated to dryness, and the entire residue was applied to the TLC plate for this experiment. However, no phosphate positive spots were found for the IAM.PC^{C12} guard column in a similar experiment. Perfusion of IAM guard columns (previously perfused with 100 mL of $CHCl_3$/MeOH (2:1 v/v)) with 0.1% (v/v) TFA/CH_3CN caused no detectable lipid leaching except for IAM.PC. For IAM.PC, significant amounts of MMPC leached during perfusion with 0.1% TFA/CH_3CN. Both IAM.PC and IAM.PC.MG showed that only fatty acids eluted from all IAM guard columns perfused with 0.1% TFA/CH_3CN. Leaching of fatty acids and MMPC is the result of cleaving the interfacial ester groups (Scheme I, sites 2 and 4), and we have recently completed the synthesis of IAM surfaces comprised of ether lipids that eliminated the instability caused by these ester groups (C. Pidgeon, unpublished results).

^{1}H NMR data corroborate the TLC, MS, and infrared data discussed above regarding the stability of IAM.PC^{C12}. ^{1}H NMR spectra of the D_2O aqueous filtrate from silica propylamine are shown in Figure 6A, and the peak assignments are shown in Scheme I. Protons of $SiOCH_2CH_3$ (peak b, δ = 1.167 ppm; peak e, δ = 3.64 ppm) and $SiCH_2CH_2CH_2$ (peak a, δ = 0.63 ppm; peak c, δ = 1.17 ppm; peak d, δ = 2.96 ppm) are apparent in the ^{1}H NMR spectra. These NMR peaks are due to the hydrolysis of Si–O–Si siloxane bond, which covalently links the silylation reagent to the silica surface (site 1a in Scheme I). We attribute this hydrolysis to the basic surface of silica propylamine because siloxane bonds are stable between pH 2 and 8 (*35*).

Figure 6B shows the ^{1}H NMR spectra of the D_2O aqueous filtrate (i.e., water-soluble compounds) and of the organic extract (i.e., organic-soluble compounds) from IAM.PC.MG. The ^{1}H NMR D_2O aqueous filtrate spectra of IAM.PC.MG do not contain silica propylamine proton signals (compare parts A and B of Figure 6). However, the D_2O aqueous filtrate spectra of IAM.PC.MG contain the MG hydrolysis product, which is glycolic acid. The methylene protons (peak p, δ = 4.12 ppm) of glycolic acid were unexpectedly intense relative to all other proton signals; consequently, the MG spectra were scaled to one-sixth the size of the other spectra in Figure 6. Leached glycolic acid may be due to hydrolysis of the immobilized MG amide link or alternatively from hydrolysis of the polymeric MG "new ester" (Scheme II). Hydrolysis of these MG amides or MG esters is expected to cause an acidic aqueous phase, and the aqueous filtrate of IAM.PC.MG had a measured pH of 2.97.

In addition to the glycolic acid peak, two choline methyl peaks (peak j, δ = 3.15 and 3.18 ppm) are apparent in the IAM.PC.MG D_2O aqueous filtrate (Figure 6B). Aqueous ^{1}H NMR spectra of GPC and MMPC demonstrated that a 0.03 ppm difference existed between the choline methyl groups of these compounds (not shown), and therefore, it is likely that at least two phospholipids leached from IAM.PC.MG to generate two choline methyl signals. However, no fatty acid protons signals are present in the region between 0.5 and 2.5 ppm, which indicates that only GPC is present in the D_2O aqueous filtrate of IAM.PC.MG. We speculate either that (i) two lipid species containing the PC headgroup leached or (ii) the GPC headgroup migrated to the adjacent glycero carbon. Nevertheless, both glycolic acid and GPC are present in the D_2O aqueous filtrate of IAM.PC.MG after a brief exposure to this aqueous solvent.

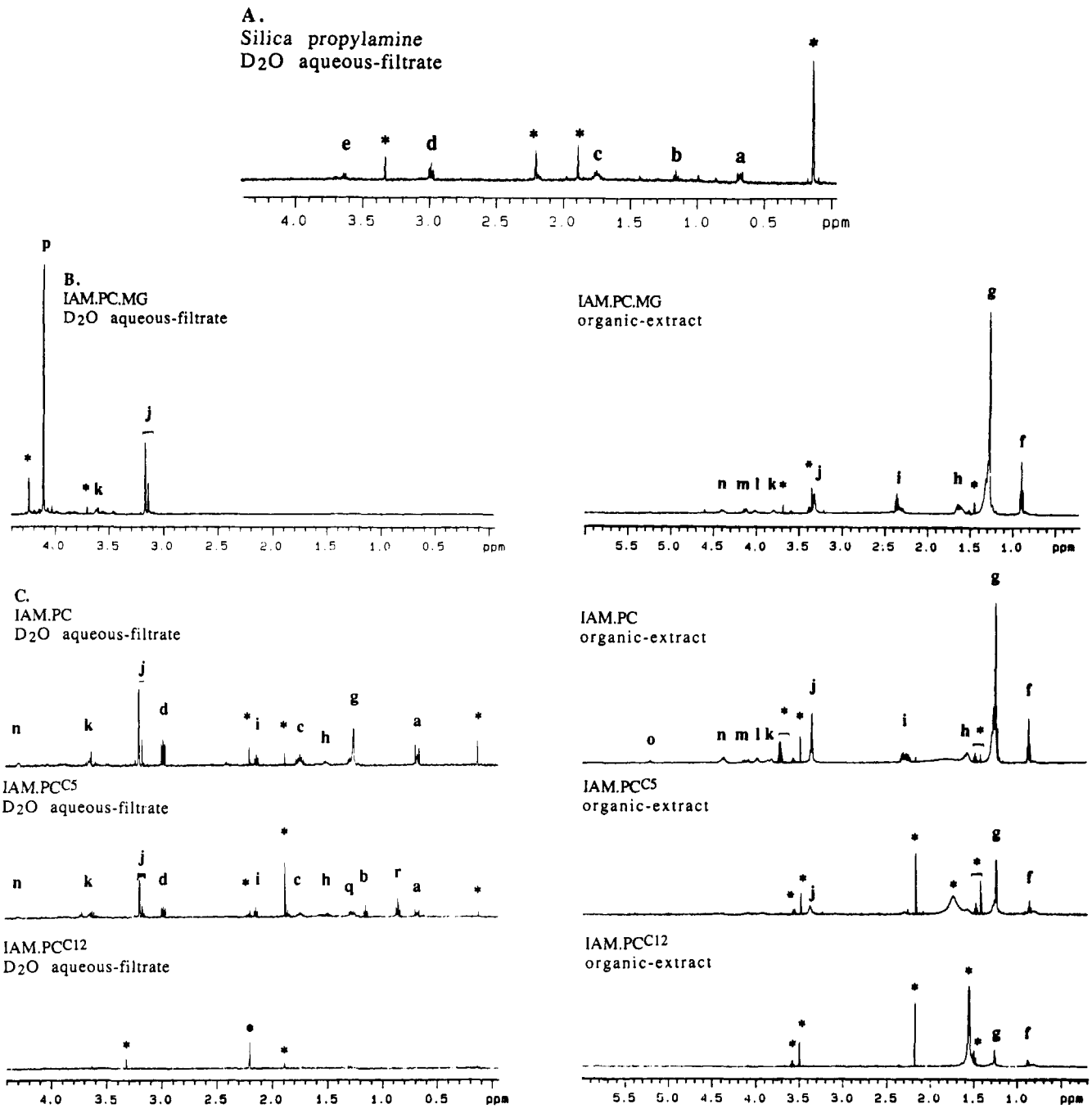

Figure 6. ^{1}H NMR (500-MHz) spectra of leached compounds from (A) silica propylamine, (B) IAM.PC.MG, and (C) IAM.PC^{C5} and IAM.PC^{C12}. Peak assignments are shown on the immobilized ligands in Scheme I. Solvent impurities and unknowns are indicated by *.

Extracting the IAM.PC.MG surface with organic solvents causes lipid leaching. Thus, extracting IAM.PC.MG surfaces previously challenged with D_2O removes lipids cleaved during the D_2O wash, but based on TLC results, at least four lipids leach into the organic extract; lecithinCOOH, lecithinCO-OCH_3, MMPC, and myristic acid. All of the proton signals of these lipids are found in the ^{1}H NMR spectra of the organic extracts: $\omega(CH_3)$ (peak f, δ = 0.88 ppm), $(CH_2)_n$ (peak g, δ = 1.26 ppm), $\alpha(CH_2)$ (peak i, δ = 2.34 ppm), $\beta(CH_2)$ (peak h, δ = 1.58 ppm), choline methyl (peak j, δ = 3.32 ppm), choline methylenes (peak k, δ = 3.76 ppm; peak n, δ = 4.40 ppm), glycerol methylenes (peak m, δ = 4.02 ppm; peak l, δ = 4.12 ppm). The glycerol methine proton was not apparent (δ = 5.20 ppm) in Figure 6B because the amount of lipid that leached was very small.

Figure 6C shows both the D_2O aqueous filtrate and organic extract ^{1}H NMR spectra of IAM.PC, IAM.PC^{C5}, and IAM.PC^{C12}. It is apparent from both the aqueous filtrate and organic extract ^{1}H NMR spectra that IAM.PC exhibits the most leaching, whereas IAM.PC^{C12} exhibits the least amount of lipid leaching. The relative intensity of all peaks in Figure 6C can be directly compared because the spectra were scaled to an external standard. Silica propylamine resonances (peaks a, c, and d) are present in the aqueous filtrate of IAM.PC and IAM.PC^{C5} but not IAM.PC^{C12}. Both IAM.PC^{C5} and IAM.PC^{C12} contain approximately 10–15% residual amines (Table II). Thus, end capping IAM.PC with the C5 anhydride did not prevent the solvolysis of unreacted silica propylamines on the IAM surface (site 1a, Scheme I), whereas end capping with the C12 anhydride prevented this solvolysis. End capping IAM.PC with the C12 anhydride prevents hydrolysis of residual silica propylamine groups on IAM surfaces exposed to nonbuffered aqueous solutions.

In addition to the silica propylamine peaks present in the

aqueous filtrate spectra of IAM.PC and IAM.PC^{C5}, other lipid peaks are present (Figure 6C). Interestingly, both the IAM.PC and IAM.PC^{C5} aqueous filtrate spectra show proton signals due to the fatty acid methylenes (peaks g, h, and i), choline methyls (peak j), and choline methylenes (peaks k and n); however, no proton signal due to the $\omega(CH_3)$ group (δ = 0.89 ppm) is present. This is consistent with the formation of spot 2 (Figure 5), which generates a lysolecithin with a terminal carboxyl group. Both the choline methyl and methylene protons are expected in the NMR without the ω CH_3 signal. In addition, multiple bond cleavage from site 3 and site 4 would generate 1,12 dodecanedicarboxylic acid, and MMPC, a lysolecithin with a terminal methyl group. During the D_2O wash step to obtain the aqueous filtrate, MMPC would remain associated with the IAM surface but the dicarboxylic acid (1,12-dodecanedicarboxylic acid) would partition from the surface, causing an increased methylene peak intensity (peaks g, h, and i). In addition, the C5 fatty acid moiety, used to end cap residual propylamines, leached from the IAM.PC^{C5} surface. This is indicated by the appearance of the C5 fatty acid $\omega(CH_3)$ group (peak r), $\alpha(CH_2)$ (peak i), $\beta(CH_2)$ (peak h), and $\gamma(CH_2)$ (peak q) in IAM.PC^{C5} aqueous filtrate ^{1}H NMR spectra (Figure 6C).

It is useful to compare peak j in the ^{1}H NMR spectra obtained from washing/extracting IAMs; peak j is the choline methyl peak, which is responsible for the phosphate positive TLC spots. The intensity of peak j is largest for the spectrum derived from IAM.PC, smaller for IAM.PC^{C5}, but absent from IAM.PC^{C12} (Figure 6C); thus, maximum chemical stability occurs after end-capping IAM.PC with C12 anhydride. In fact, ^{1}H NMR spectra of both the organic extract and aqueous filtrate of IAM.PC^{C12} show predominantly solvent impurities. Labeled with a *, the solvent impurities in the aqueous filtrate spectra include δ = 3.42 ppm, MeOH; δ = 2.20 ppm, acetone; and δ = 1.90 ppm, CH_3CN, and the solvent impurities in the organic extract spectra include δ = 3.60 and 1.50 ppm, ethyl chloride; δ = 3.49 ppm, methanol; δ = 2.18 ppm, acetone; and δ = 1.56 ppm, water. Because choline methyl protons were absent in the IAM.PC^{C12} organic extract spectra, the low-intensity NMR signals (peaks f and g) are from trace amounts of leached fatty acid. For the other IAM packing materials, unknown impurities also occur in both the aqueous filtrate spectrum (IAM.PC.MG δ = 3.71 and 4.24 ppm), and organic extract spectrum (IAM.PC.MG, δ = 1.45, 3.35, and 3.70 ppm; IAM.PC, δ = 1.42 and 3.65 ppm; IAM.PC^{C5}, δ = 1.42 ppm). We note that we are evaluating trace amounts (<1 μmol) of ligands that leached, which permit solvent impurities to appear with similar peak intensities.

DISCUSSION

IAM.PC, IAM.PC.MG, and IAM.PC.glycidol packing materials rapidly wet when suspended in aqueous solvents. In contrast, end capping IAM.PC with anhydrides containing C3–C12 chain lengths decreases the ability of the IAM.PC particles to wet when suspended in aqueous solvents. Because all purification strategies of membrane protein using IAM surfaces will include detergents (or organic solvents) in the mobile phase, the wettability of the surface is not critical for protein purification. However, the decreased wettability of IAM particles end capped with anhydrides suggests that the increased hydrocarbon loading significantly altered the hydrophobicity of the surface. If a monolayer of tightly packed phospholipid molecules were covalently bonded to the IAM.PC surface, then one would not expect the wettability of the surface to change after end capping with anhydrides. A tightly packed monolayer of membrane lipids would provide a monolayer of hydrophilic headgroups projecting away from the IAM surface, and these surfaces are expected to easily wet. Thus, we speculate that the molecular density of immobilized phospholipids on IAM bonded phases prepared to date is less than the phospholipid packing density in artificial membranes. However, we note that the phospholipid packing density in artificial membranes is high because lipid molecules have lateral mobility in this lipid system. In contrast, immobilized lipids lack lateral mobility and cannot be expected to exhibit the same molecular packing properties.

Previously, we reported that IAM.PC surfaces leach hydrocarbon when challenged with common HPLC mobile phases (*8*, *9*, *12*). From the results of this present study, the most vulnerable bond is the amide link shown in Scheme I. This was unexpected because esters are significantly more labile than amides, and consequently, the PC esters should have been the most vulnerable bond. The putative mechanism for increased lability of the amide link involves hydrogen bonding of the amide link with the silica unreacted surface amines (*8*, *9*, *12*). Unreacted surface propylamines also contribute to the chemical instability of the IAM phase by making the silica subsurface basic. We are pursuing several studies (^{31}P NMR, enzyme reconstitution, chemical synthesis, etc.) using IAM surfaces not packed in columns, and for these studies, it is necessary to have IAM surfaces that do not exhibit any lipid leaching.

From a chromatographers point of view, lipid leaching from non-end-capped IAM.PC columns is marginally acceptable. For example, 2000 mL of pH 7.2 citric acid buffer caused 0.08% HC loss from an initial 3.98% HC loading (*8*). This corresponds to a leaching rate of approximately 2% of the immobilized lipid per 2000 mL of mobile phase (0.08% HC/3.98% HC × 100 = 2%). IAM.PC contains approximately 50–60 mg of PC/g of packing material, and 2000 mL of this buffer volume thus causes approximately 1 mg of lipid/g of packing material to be lost. This amount of leaching is marginally acceptable for chromatographic work (*3–7*) but severely limits the column lifetime. Although column lifetime is limited, a single IAM.PC HPLC column was used 20–30 times over 2–3 years for the purification of cytochrome P450 isozymes (*6*). Thus, lipid leaching does not prohibit using the IAM.PC column for chromatographic purposes; however, leaching does prohibit using the IAM.PC packing material for nonchromatographic studies (^{31}P NMR, enzyme reconstitution, chemical synthesis, etc.) presently in progress in our lab.

Increasing the alkyl chain length on reversed-phase packing material increases the column lifetime by preventing the solvolysis of the silica surface (*36*). The mechanism for increased column lifetimes is attributed to the decreased solvent accessibility to the silica surface. Similarly, our strategy for end capping the IAM surface was to fill the surface interphase with hydrocarbon to decrease the solvent accessibility of mobile-phase molecules to the silica surface. End capping with small molecules eliminates the chemically basic subsurface (i.e., the major cause for chemical degradation of the IAM surface), but solvent molecules can penetrate the IAM interfacial region, allowing solvolysis of the silica surface to occur. Thus, increasing the hydrocarbon content *in* the IAM monolayer, using long alkyl chains, was expected to both eliminate the amines (i.e., eliminate the chemically basic subsurface) and decrease the solvent accessibility to the silica surface. The steric protection of the Si–O–Si groups on the silica surface was shown to be critical for preparing very stable reversed-phase bonded phases (*37*). Increasing the hydrocarbon content of the IAM interphase provides steric protection of the silica surface and prevents solvent molecules from reaching the silica surface.

ACKNOWLEDGMENT

C. Pidgeon gratefully acknowledges the support of NSF (CTS 8908450) and Eli Lilly and Company. Support for Xiaoxing Qiu is provided by Schering-Plough. Dave E. Nichols

is supported by DA 02189 from the National Institute of Drug Abuse. The technical support of Joan Stevens, Helen O'-Connel, and Jean Shaw is greatly appreciated.

LITERATURE CITED

(1) Pidgeon, C. Immobilized Artificial Membrane. U.S. Patent 4,931,498, 1990.
(2) Pidgeon, C. Method for Solid Membrane Mimetics. U.S. Patent 4,927,879, 1990.
(3) Thurnhofer, H.; Schnabel, J.; Betz, M.; Lipka, G.; Pidgeon, C.; Hauser, H. *Biochim. Biophys. Acta* **1991**, *1064*, 275–286.
(4) Chae, W. G.; Luo, C.; Rhee, D. M.; Lombardo, C. R.; Low, P.; Pidgeon, C. Immobilized Artificial Membrane Chromatography: Initial Studies using monomyristoylphosphatidylcholine as a detergent for solubilizing and purifying membrane proteins. *Mod. Phytochem. Methods* **1991**, *25*, 149–174.
(5) Otto, S.; Marcus, C.; Pidgeon, C.; Jefcoat, C. *Endocrinology* **1991**, *129*, 970–982.
(6) Pidgeon, C.; Stevens, J.; Otto, S.; Jefcoate, C.; Marcus, C. *Anal. Biochem.* **1991**, *194*, 163–173.
(7) Pidgeon, C.; Venkatarum, U. V. *Anal. Biochem.* **1989**, *176*, 36–47.
(8) Markovich, R. J.; Stevens, J. M.; Pidgeon, C. *Anal. Biochem.* **1989**, *182*, 237–244.
(9) Stevens, J. M.; Markovich, R. J.; Pidgeon, C. *BioChromatography* **1989**, *4*, 192–205.
(10) Pidgeon, C. *Enzyme Microb. Technol.* **1990**, *12*, 149–150.
(11) Pidgeon, C.; Apostol, G.; Markovich, R. *Anal. Biochem.* **1989**, *181*, 28–32.
(12) Markovich, R. J. Ph.D. Dissertation, Purdue University, West Lafayette, IN, 1990.
(13) White, R. L.; Nair, A. *Appl. Spectrosc.* **1990**, *44*, 69–75.
(14) Leyden, D. E.; Murthy, R. S. S. *Spectroscopy* **1987**, *2* (2), 28–36.
(15) Graf, R. T.; Koenig, J. L.; Ishida, H. *Anal. Chem.* **1984**, *56*, 773–778.
(16) Mckenzie, M. T.; Culler, S. R.; Koenig, J. L. *Appl. Spectrosc.* **1984**, *38*, 786–790.
(17) Mckenzie, M. T.; Koenig, J. L. *Appl. Spectrosc.* **1985**, *39*, 408–412.
(18) Murthy, R. S. S.; Leyden, D. E. *Anal. Chem.* **1986**, *58*, 1228–1233.
(19) Murthy, R. S. S.; Blitz, J. P.; Leyden, D. E. *Anal. Chem.* **1986**, *58*, 3167–3172.
(20) Blitz, J. P.; Murthy, R. S. S.; Leyden, D. E. *Appl. Spectrosc.* **1986**, *40*, 829–831.
(21) Blitz, J. P.; Murthy, R. S. S.; Leyden, D. E. *J. Colloid Interface Sci.* **1988**, *121*, 63–69.
(22) Scott, D. L.; Otwinowski, Z.; Gelb, M. H.; Sigler, P. B. *Science* **1990**, *250*, 1463–1566.
(23) Griffiths, P. R.; Fuller, M. P. *Adv. Infrared Raman Spectrosc.* **1982**, *9*, 63–129.
(24) Fraser, D. J. J.; Griffiths, P. R. *Appl. Spectrosc.* **1990**, *44*, 193–199.
(25) Yeboah, S. A.; Wang, S. H.; Griffiths, P. R. *Appl. Spectrosc.* **1984**, *38*, 259–264.
(26) Hamadeh, I. M.; Yeboah, S. A.; Trumbull, K. A.; Griffiths, P. R. *Appl. Spectrosc.* **1984**, *38*, 486–491.
(27) Christy, A. A.; Tvedt, J. E.; Karstang, T. V.; Velapoldi, R. A. *Rev. Sci. Instrum.* **1988**, *59* (3), 423–426.
(28) Tevrucht, M. L. E.; Griffiths, P. R. *Appl. Spectrosc.* **1989**, *43*, 1492–1494.
(29) Olinger, J. M.; Griffiths, P. R. *Anal. Chem.* **1988**, *60*, 2427–2435.
(30) Fraser, D. J. J.; Norton, K. L.; Griffiths, P. R. *Anal. Chem.* **1990**, *62*, 308–310.
(31) Hair, M. L. Transmission Infrared Spectroscopy for High Surface Area Oxides. *Vibrational Spectroscopy For Absorbed Species*; American Chemical Society: Washington, DC, 1980; pp 1–11 and references therein.
(32) Ihler, R. K. The Surface Chemistry of Silica. *The Chemistry of Silica: Stability, Polymerization, Colloid & Surface Properties, and Biochemistry*; Wiley and Sons: New York, 1979; pp 623–729 and references therein.
(33) Ferraro, J. R.; Manghnani, M. H.; Quattrochi, A. *Phys. Chem. Glasses* **1972**, *13* (4), 116–121.
(34) Pluckthun, A.; Dennis, E. A. *Biochemistry* **1982**, *21*, 1743–1750.
(35) Snyder, L. R.; Kirkland, J. J. *Introduction to Modern Liquid Chromatography*; Wiley and Sons: New York, 1989; pp 270–322.
(36) Hetem, M. J. J.; de Haan, J. W.; Claessens, H. A.; van de Ven, L. J. M.; Cramers, C. A. *Anal. Chem.* **1990**, *62*, 2288–2296.
(37) Kirkland, J. J.; Glajch, J. L.; Farlee, R. D. *Anal. Chem.* **1989**, *61*, 2–11.

RECEIVED for review February 20, 1991. Accepted May 17, 1991.